

Supplementary Material

Supplementary Table S1: Strains used in this study

Strain	Genotype	Reference
MAD973	<i>yA2, pabaA1, argB2, pacC^C700</i>	CIB's stock collection
MAD1132	<i>wA3, sltA1, pantoB100</i>	CIB's stock collection
MAD1445	<i>yA2, pabaA1, pacC^C14900</i>	Hervás-Aguilar et al., (2007)
MAD1652	<i>yA2, pabaA1, pacX20, pacC900</i>	Bussink et al.,(2015)
MAD1775	<i>pyrG89, pyroA4, inoB2, nkuAΔ::bar, palBΔ::pyroA, pacC900</i>	CIB's stock collection
MAD1929	<i>pyroA4, pacX-gfp, hhoA-mrfp, riboB2</i>	CIB's stock collection
MAD2352	<i>wA4, pyrG89, pyroA4, inoB2, nkuAΔ::bar, palF::ha₃::pyrG^{Af}, pacC900</i>	Bussink et al.,(2015)
MAD3367	<i>pantoB100, vps23::gfp::pyrG^{Af}</i>	Galindo et al., (2012)
MAD3369	<i>pyroA4, palF15, vps23::gfp::pyG^{Af}</i>	Galindo et al., (2012)
MAD3419	<i>inoB2, pacC900, sltA60</i>	CIB's stock collection
MAD3652	<i>pyrG89, pabaA1, argB2, nkuAΔ::argB, sltA::ha₃::pyrG^{Af}, riboB2</i>	Mellado et al., (2016)
MAD3693	<i>pyrG89, pabaA1, argB2, nkuAΔ::argB, sltA::ha₃::pyrG^{Af}, riboB2, sltBΔ::riboB^{Af}</i>	Mellado et al., (2016)
MAD3816	<i>sltAΔ::pyrG^{Af}, pyroA4, riboB2, argB2, nkuAΔ::argB</i>	Mellado et al., (2016)
MAD3919	<i>pyrG89, pabaB22, nkuAΔ::argB (argB2), sltA::ha₃::riboB^{Af}, riboB2</i>	Mellado et al., (2015)
MAD4296	<i>yA2, biA1, pabaA1, pyrG89, sltAΔ::pyrG^{Af}, argB2, pacC^C14900</i>	Mellado et al., (2016)
MAD4499	<i>pabaA1, pantoB100, pyroA4:[gpdA^{mini}::palF (cDNA)::ha₃::ub::pyroA^{trunc}], pacC900</i>	CIB's stock collection
MAD5736	<i>pyrG89, pyroA4</i>	CIB's stock collection
MAD6669	<i>pyrG89, pabaB22, nkuAΔ::argB(argB2), riboB2, sltA::ha₃::riboB^{Af}</i>	Picazo et al., (2020)
MAD7621	<i>nkuAΔ::argB(argB2)?, sltAΔ::pyrG^{Af}, pacX20</i>	This work. From cross MAD3816 x MAD1652
MAD7622	<i>wA3, sltA1, pacX20</i>	This work. From cross MAD1132 x MAD1652
MAD7623	<i>yA2, pyrG89?, pabaA1?, pabaB22?, nkuAΔ::argB(argB2)?, sltBΔ::riboB^{Af}, sltA::ha₃::pyrG^{Af}, pacX20, pacC900, riboB2?</i>	This work. From cross MAD3693 x MAD1652
MAD7624	<i>nkuAΔ::argB(argB2)?, pacX20, sltA::ha₃::riboB^{Af}</i>	This work. From cross MAD6669 x MAD1652
MAD7625	<i>pyrG89?, pyroA4, nkuAΔ::argB(argB2)?, sltAΔ::riboB^{Af}, pacX-gfp, hhoA-mrfp, riboB2?</i>	This work. From cross MAD1929 x MAD3919

MAD7626	<i>pyrG89?</i> , <i>pyroA4</i> , <i>nkuAΔ::argB(argB2)?</i> , <i>pacX-gfp</i> , <i>hhoA-mrfp</i> , <i>riboB2</i>	This work. From cross MAD1929 x MAD3919
MAD7627	<i>wA4</i> , <i>nkuAΔ::argB(argB2)?</i> , <i>nkuAΔ::bar?</i> , <i>pacC900</i> , <i>palF500</i>	This work. From cross MAD7621 x MAD2352
MAD7628	<i>pyroA4</i> , <i>inoB2</i> , <i>nkuAΔ::argB(argB2)?</i> , <i>nkuAΔ::bar?</i> , <i>pacX20</i> , <i>pacC900</i> , <i>palF500</i>	This work. From cross MAD7621 x MAD2352
MAD7629	<i>wA4</i> , <i>pyroA4</i> , <i>nkuAΔ::argB(argB2)?</i> , <i>nkuAΔ::bar?</i> , <i>sltAΔ::pyrG^{Af}</i> , <i>pacX20</i> , <i>pacC900</i> , <i>palF500</i>	This work. From cross MAD7621 x MAD2352
MAD7630	<i>pyroA4</i> , <i>nkuAΔ::argB(argB2)?</i> , <i>nkuAΔ::bar?</i> , <i>sltAΔ::pyrG^{Af}</i> , <i>pacC900</i> , <i>palF500</i>	This work. From cross MAD7621 x MAD2352
MAD7631	<i>wA4</i> , <i>pyroA4</i> , <i>inoB2</i> , <i>nkuAΔ::argB(argB2)?</i> , <i>nkuAΔ::bar?</i> , <i>sltAΔ::pyrG^{Af}</i> , <i>pacC900</i>	This work. From cross MAD7621 x MAD2352
MAD7632	<i>pyroA4</i> , <i>pabaA1</i> , <i>nkuAΔ::argB(argB2)?</i> , <i>argB2?</i> , <i>pacC^C700</i> , <i>riboB2</i>	This work. From cross MAD973 x MAD3816
MAD7633	<i>yA2</i> , <i>pyroA4</i> , <i>pabaA1</i> , <i>nkuAΔ::argB(argB2)?</i> , <i>argB2?</i> , <i>sltAΔ::pyrG^{Af}</i> , <i>pacC^C700</i> , <i>riboB2</i>	This work
MAD7634	<i>wA4</i> , <i>inoB2</i> , <i>nkuAΔ::argB(argB2)?</i> , <i>nkuAΔ::bar?</i> , <i>sltAΔ::pyrG^{Af}</i> , <i>pacC900</i> , <i>pyroA4::[gpdA^{mini}::palF (cDNA)::ha₃::ub::pyroA^{trunc}]</i>	This work
MAD7669	<i>pyrG89</i> , <i>pyroA4</i> , <i>nkuAΔ::bar</i> , <i>vps23::gfp::pyrG^{Af}</i>	This work
MAD7670	<i>pyrG89</i> , <i>pabaB22</i> , <i>nkuAΔ::bar</i> , <i>sltAΔ::ribob^{Af}</i> , <i>riboB2</i> , <i>vps23::gfp::pyrG^{Af}</i>	This work
MAD7671	<i>wA3</i> , <i>pantoB100</i> , <i>pacC900</i> , <i>pacX20</i> , <i>sltA1</i>	This work. From cross MAD1132 x MAD1652
MAD8108	<i>pyrG89</i> , <i>nkuAΔ::bar</i> , <i>pyroA4,inoB2</i> , <i>palBΔ::pyroA</i> , <i>sltAΔ::pyrG^{Af}</i>	This work

Supplementary Table S2: Oligonucleotides used in quantitative PCR experiments

Primer	Sequence (5'-3')
qPCR_sltA_1	TCCTCAGCAACAGACTACCTCGC
qPCR_sltA_2	CAAGATCGAACGGTTAGACGG
qPCR_sltB_1	ATCAACCAGGATCGCTTAGACGC
qPCR_sltB_2	GTACGTTACCATCGTCAACGC
qPCR_pacC_1	CTACATTGCCAACCGTCTTGAGC
qPCR_pacC_2	GGGATACATCACACTGTCTCGG
qPCR_palF_1	CTCTTGCCTAGTCAACCTCCGTG
qPCR_palF_2	CGCTCCAACCTCTGTTATCCTC
qPCR_pacX_1	TCAGCAGTAAGGGAGGTGTCTCC
qPCR_pacX_2	GATCCTGATCCCGCTCCATATC
qPCR_benA_1	AGATGCGAACATCCAGAGC
qPCR_benA_2	CTGGTACTCGGAGACGAGATCG

Supplementary figures

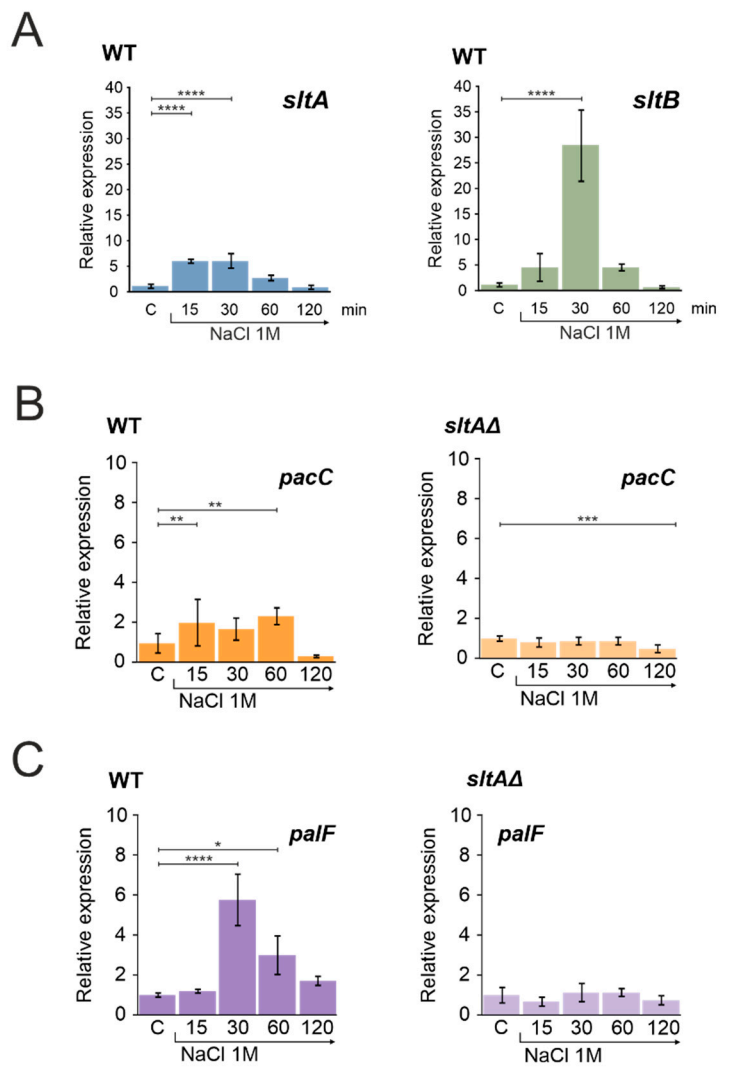
Figure S1: Gene expression profiles in wild-type and *s/tAΔ* strains grown under stress caused by high extracellular sodium concentration. A) Expression profiles of *s/tA* and *s/tB* genes in mycelia of wild-type strain grown in standard culture condition (Control, C) and then transferred to medium containing 1 M NaCl. Panels B and C show the expression levels of *pacC* (B) and *palF* (C) genes in mycelia from wild-type and null *s/tA* strains grown in non-stressing condition (Control, C) and in the presence of 1 M NaCl. Wild-type and null *s/tA* strains used in this experiment were MAD3652 and MAD3816, respectively. Error bars represent the standard deviations of three replicates for each sample result. *, P<0.01-0.05; **P<0.001-0.01; ***,P<0.0001-0.001; ****, P<0.00001. Not significant P-values (≥ 0.05) are not indicated in graphs.

Figure S2: Patterns of PacC proteolysis at alkaline pH along extended experimental times and with calcium supplementation. A) Detection of PacC forms in ambient alkaline pH along 4 hours in wild-type and *s/tAΔ* strains. Strains and methodology used are the same as in Figure 2. Exploring longer experimental times aimed to detect a delayed proteolytic processing of PacC^{72kDa} after medium alkalinisation in the absence of SltA activity. B) Similarly, the effect of 10 mM CaCl₂ was studied on the pattern of proteolytic processing of in the wild-type and null *s/tA* backgrounds. Neither longer exposure to alkaline pH nor addition of calcium modified the pattern of PacC proteolysis observed in the null *s/tA* mutant. C) Detection of PacC protein forms in the *s/tA60* mutant background (MAD3419) at alkaline pH. The mild loss-of-function phenotype caused by *s/tA60* allele allowed the detection of PacC^{53kDa} form and recovered higher levels of PacC^{27kDa} with a correct electrophoretic mobility although notable levels of PacC^{72kDa} were observed compared to a wild-type background (see text for details).

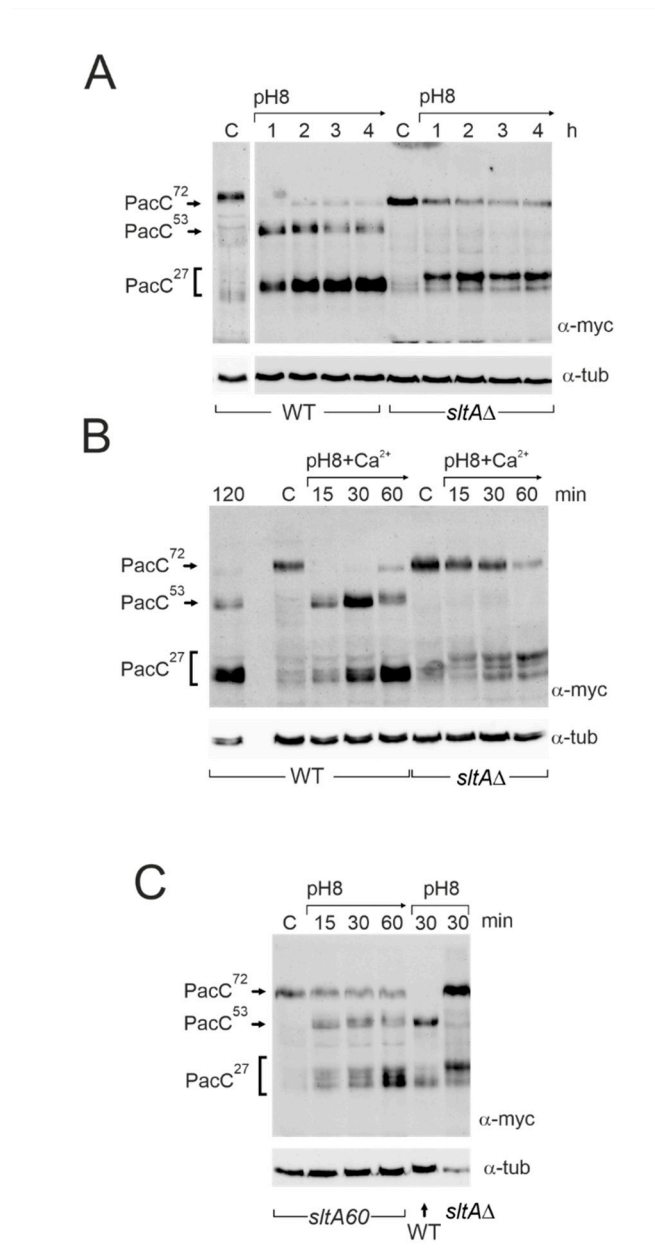
Figure S3: Characterization of the zinc binuclear cluster protein PacX. A) Analysis of expression levels of PacX-GFP and degradation forms in WT and null *sltA* background at pH 8. On the right, relative quantification of protein levels of PacX and degraded PacX (PacX deg). B) *In vivo* detection of PacX-GFP protein by fluorescence microscopy. Nuclei were detected by tagging histone 1 (HhoA) with monomeric red fluorescent protein (mRFP). Cells were visualised in control condition and after 15 and 120 minutes of alkalinity induction. PacX-GFP cellular localisation was not altered in any strain or condition tested.

Figure S4: Effects of *pacX20* mutation in PacC protein levels and proteolytic processing. A) Comparative immunodetection of PacC forms in *wild-type*, *sltAΔ* (top) and *pacX20* single mutants and the double mutant *sltAΔ pacX20* (bottom). Exposure times were comparable and images highlight the positive effect of *pacX20* mutation on PacC levels. B) Lack of effect of *pacX20* mutation on the incorrect processing of PacC in *sltAΔ*, *sltBΔ* and *sltA1* mutant backgrounds.

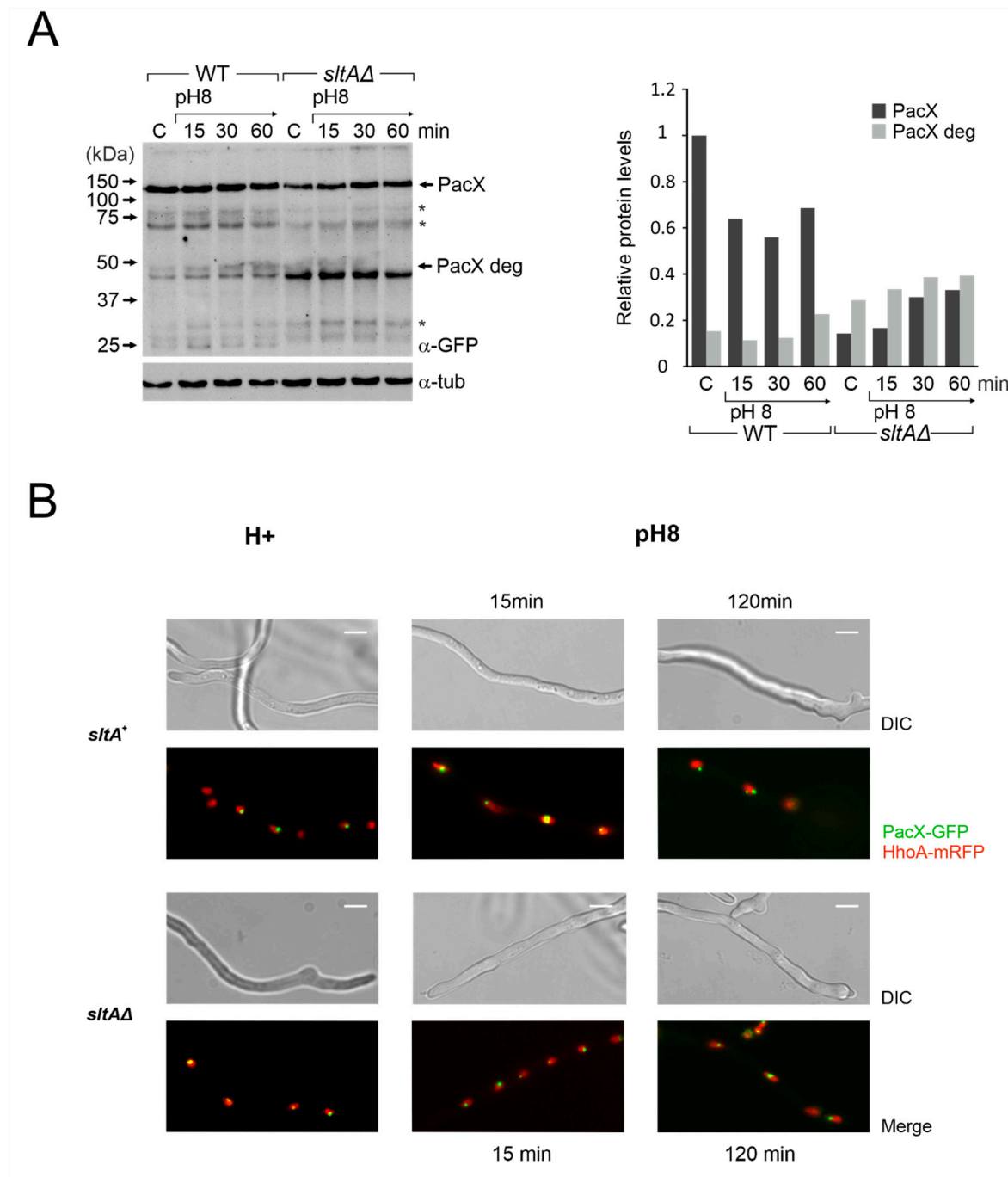
FigureS1



FigureS2

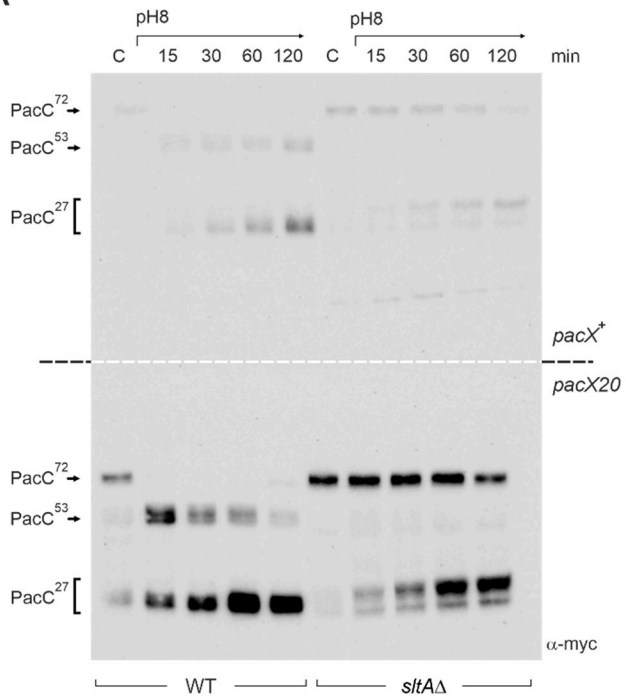


FigureS3



FigureS4

A



B

